International Journal of Modern Manufacturing Technologies
ISSN 2067–3604, Vol. XV, No. 2 / 2023
https://doi.org/ 10.54684/ijmmt.2023.15.2.111

THE EFFECT OF CASTING PARAMETERS ON THE MICROSTRUCTURE AND CORROSION BEHAVIOR OF SAE 430B ALLOYS FOR TRANSPORTATION INDUSTRY

Nicoleta - Monica Lohan[1], Ioan Carcea[2], Bogdan Pricop[1], Mihail Sârghi[2], Nicanor Cimpoeșu[1], Mihai Popa[1], Costică Bejinariu[1], Ancuța - Elena Ciorobatca[2], Diana - Petronela Burduhos-Nergiș[1]

[1]"Gheorghe Asachi" Technical University of Iasi, Faculty of Materials Science and Engineering, Blvd Dimitrie Mangeron 41, 700050 Iași, Romania
[2] SC RANCON SRL, str. George Cosbuc, nr. 25, Iasi, Romania

Corresponding author: Bogdan Pricop, pricop.bogdan@academic.tuiasi.ro

Abstract: SAE 430B is a Cu-based alloy, which, due to good properties qualify the alloy in special bronzes category. In this paper, the influence of the casting parameters on the properties of the SAE 430B cast in two types of moulds: (i) temporary (based on quartos sand) and (ii) permanent (metallic mould). Samples in as-cast condition were cut and prepared for chemical and microstructural analysis. The chemical composition was determined via spectroscopic analysis, the structural characterization was carried out by optical and electronic microscopy. EDS chemical analysis was used to identify the compositions of phases and compounds in the material. The corrosion behaviour was analysed in seawater by a linear potentiodynamic polarization test. The microstructure of as-cast samples presents a β phase structure with intermetallic precipitates with various morphologies. With the increase in cooling rate, corrosion potential values become more negative and current density increases.
Key words: *SAE 430B alloy, casting, cooper alloy, microstructure, corrosion behaviour.*

1. INTRODUCTION

SAE 430B is a Cu-based alloy obtained from CuZn25 brass by adding Al, Fe and Mn. The structure and properties acquired because of alloying, positions the SAE 430B alloy in the special bronzes category due to good mechanical, chemical and technological properties. It contains Cu (60–66%), Zn (22-28%), Al (3.0–7%), Fe (2,0–4,0%), Mn (2,5–5%) and a small amount of Sn, Pb, P and Sb, in accordance with SR EN 1982:2008 Copper and copper alloys - Ingots and castings standard [1]. The addition of more than 3.5% aluminum leads to an increase in both strength and fluidity [2]. Iron improves toughness, splinterability and causes a finer structure. Manganese improves the yield strength, tensile strength, relative elongation and corrosion resistance in seawater. The layer of protective oxides ensures the corrosion resistance of these alloys [3]. Alloying with 5 up to 7% Al lowers phase transformation point of α to β, from 800 °C to temperatures below 700 °C. Additional alloying with Fe and Mn, which have the same influence on the structure, can lower this point even below 600°C [4].
Good mechanical strength, superior wear resistance, high thermal and electrical conductivity, as well as high corrosion resistance in various aggressive environments, including seawater, makes this alloy recommended for components in the transport industry. Applications include propellers for marine applications, bushings, bearings, gears, parts for hydraulic cylinders, butterfly valves [5, 6] and also cams, nuts, bridge pins, valve rods, bolts for road transport vehicles, parts of aircraft landing gear, pipe fittings and pipelines for the oil and gas industry [2].
Since this alloy exhibits poor weldability and deformability, is difficult to solder and cannot be heat treated [7]. Often, most parts are obtained by casting, mostly in temporary moulds [8] according to the recommendations provided in ASTM B148-18, which in term causes large variations in the microstructure of the alloy. The purpose of this paper is to analyze the relationship between the casting conditions and the chemical and structural properties of the obtained SAE 430B samples.

2. MATERIALS AND METHODS

For this study, two types of samples were analyzed: one cast in temporary (quartos sand mixture) and the second in permanent (metallic) mould. The cooling of the material in contact with the moulding sand ensures a slow heat transfer while the cooling of the material in contact with the metallic mould ensures a high cooling rate and rapid solidification, which determines a high thermal gradient. The chemical composition of the samples was determined by spectrometric analysis on the Foundry Master spectral analyzer and the results are shown in Table 1.

Table 1. Chemical composition of SAE 430B

Chemical element	Cu	Zn	Al	Fe	Mn	Si	Others
Concentrations, at%	63.0	22.5	5.21	4.14	2.6	0.5	rest

Fragments were cut by electroerosion with a Mo wire (ϕ0.18 mm) on a DEM 320 machine and prepared for microstructural and chemical analysis. Microstructural analysis was performed using optical microscopy (OM) and electron microscopy (SEM). In addition, the chemical composition of the samples was determined by EDS analysis and the corrosion properties were evaluated by linear potentiodynamic polarization. For OM, the samples were prepared manually by grinding, polishing and etching. Grinding was performed on metallographic paper with grits of 600, 800, 1000, 1200, 1500 and 2000. Polishing was carried out on a polishing cloth using two Al_2O_3 solutions of with diameters of 0.3 and 0.05μm. The etching with chemical reagent was carried out with a solution of $FeCl_3$ + HCl + distilled water. The optical microstructures were obtained using an OPTIKA XDS-3 MET optical microscope, equipped with an OPTIKAM 4083.B5 digital camera and OPTIKAM B5 software. In order to identify the nature of the existing phases and the compounds formed, as well as for microstructural analysis at a higher magnification power, SEM analyses were performed on an electron scanning microscope equipment model Vega Tescan LMH II equipped with an EDAX detector for qualitative and quantitative analysis. Considering the applications of this alloy in the shipping industry, the analysis of corrosion resistance by linear polarization was performed in seawater from the Black Sea, with a pH value of 8.37. The corrosion resistance of the two samples was determined by a linear potentiodynamic polarization test (LPDP). The equipment used is an OrigaFlex OGF+01A potentiostat (France) with a three-electrode electrochemical cell, composed of a platinum auxiliary electrode, a calomel reference electrode and a working electrode. The working electrode exposed surface was 0.502cm^2. The potentiodynamic curves were recorded for a scan rate of 0.5mV/s and a scan voltage range of ±500mV. These curves were recorded after 30 minutes immersion in the solution. All the tests were repeated three times.

3. RESULTS AND DISCUSSION

Figure 1 shows the microstructure of SAE 430 B alloy cast in temporary and permanent mould. In the case of the solidified sample in contact with the temporary form (Figure 1, a) the structure consists of solid solution β and numerous precipitates (mainly in globular form). This phase is rich in copper, has a body-centered cubic structure (BCC) and is specific to Cu-based alloys [9]. The grains are large with irregular shape, uneven in size, oriented in the direction of the thermal gradient of solidification. In the structure, numerous pores (gas bubbles) appear due to the difference in gas solubility in molten and solidified metal. The solidified sample in contact with the permanent mould has a β structure and numerous precipitates distributed mainly in the grains boundaries (Figure 1, b). At higher magnification, it can be seen that gray precipitates have rosette shapes, are fine globular or coarse. Rosette-shaped precipitates have large dimensions (5 – 10)μm and those of globular shape are smaller. A similar structure has been reported in the case of bronzes with Ni [2] where the precipitates formed were in the form of numerous, small, fine particles of globular shape but also with lamellar and rosettes morphology.
The SEM microstructure of the solidified sample in contact with the temporary mould in Figure 2(a) confirms the aspects observed on optical microscopy. The structure has large columnar grains compared to those obtained in the solidified sample in contact with the permanent mould, Figure 2(b). Slow cooling allows the obtainment of grains oriented in the direction of the thermal gradient; their length being twice their width. In both of samples structure, several ellipsoidal cavities are observed due to solidification in the temporary mould.

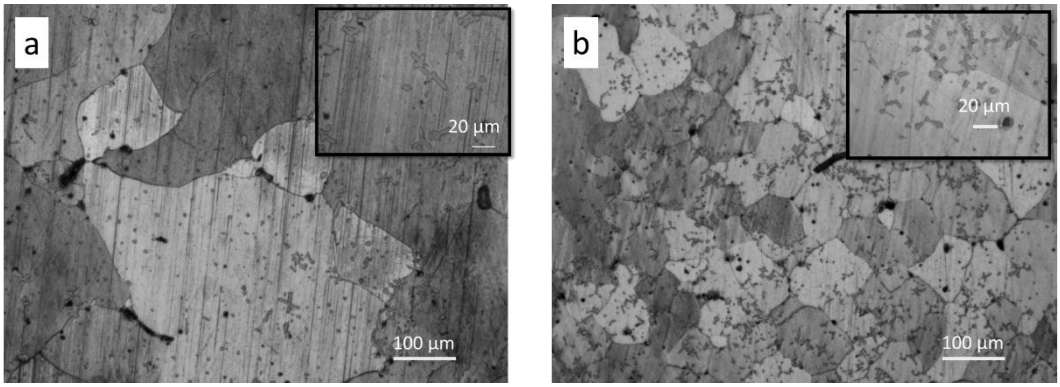

Fig. 1. OM micrographs: general aspects illustrating the grain size and detail of precipitates of as-cast SAE 430B alloy cast in: (a) temporary mould and (b) permanent mould

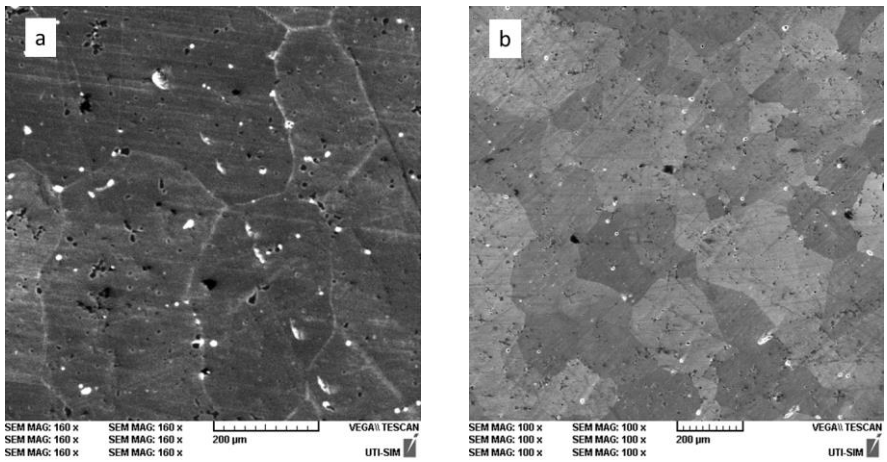

Fig. 2 SEM micrographs of as-cast SAE 430B alloy cast in: (a) temporary mould and (b) permanent mould

At higher magnification, the sample solidified in the temporary mould (Figure 3a) contains precipitates mainly of globular shape, preferentially formed on the grain limit. The sample solidified in metallic mould (Figure 3, b) exibites, at the intersection of grains, the existence of another phase. Hashemi M. called this phase α when the microstructure of the alloy SAE 430B (C86300) contains dark dendrites of α phase in a matrix of β equiaxed grains [10, 11].

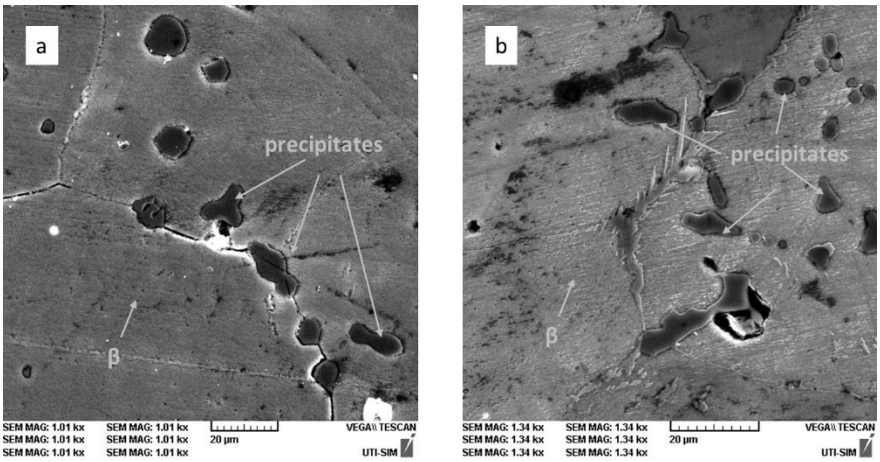

Fig 3. SEM micrographs: Detail of precipitates of as-cast SAE 430B alloy cast in: (a) temporary mould and (b) permanent mould

The quantitative determination of the chemical elements was performed by applying the POINT analysis mode, in three points marked on the three micrographs of SAE 430B alloy as shown in Figure 4. Their quantity in atomic percentage can be found in Table 2.

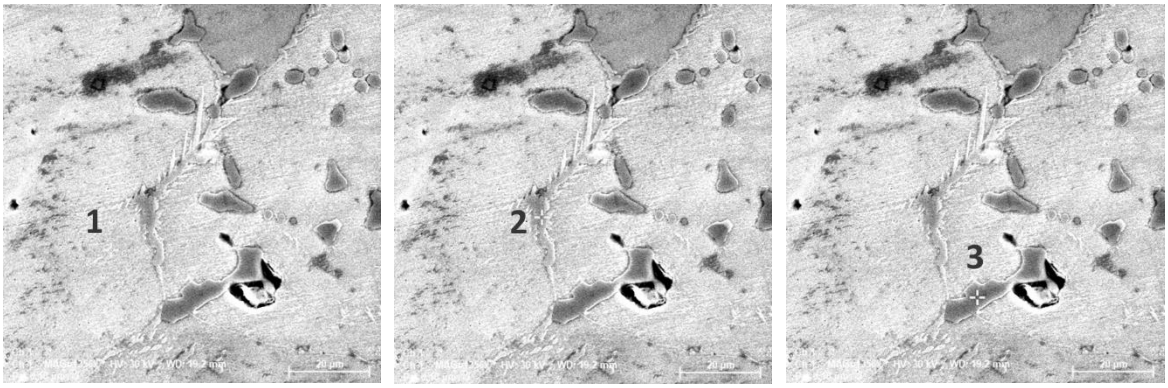

Fig. 4. Chemical analysis in POINT mode in case of SAE 430B alloy analysis

Table 2. Amount of chemical elements identified by EDS analysis

Point	Chemical elements, at%						
	Cu	Zn	Al	Mn	Fe	Si	Pb
1	61.24	21.3	13.9	3.13	-	-	0.43
2	69.8	19,12	8.76	2.32	-	-	-
3	3.34	1.21	3.22	15.65	55.15	21.43	-

EDS analyses and values in Table 2 support the above statements, the presence of β (point 1) and α (point 2) phases rich in Cu (61.24 and 69.8 % Cu, respectively) as well as Zn, Al and Mn. Point 3 corresponds to a precipitate that is rich in Fe and is characterized by precipitation within β phase. In alloyed brass these precipitates have the formula $(Fe, Mn)_5 Si_3$ and have a variable composition: their interior is enriched in iron, and the outer surface is enriched in manganese [9].
The potentodynamic curves of the tested samples are shown in Figure 5. In addition, corrosion potential values (E_{cor}), current density (I_{cor}), polarization resistance (R_p) and corrosion rate (C_R) are resented in Table 3.

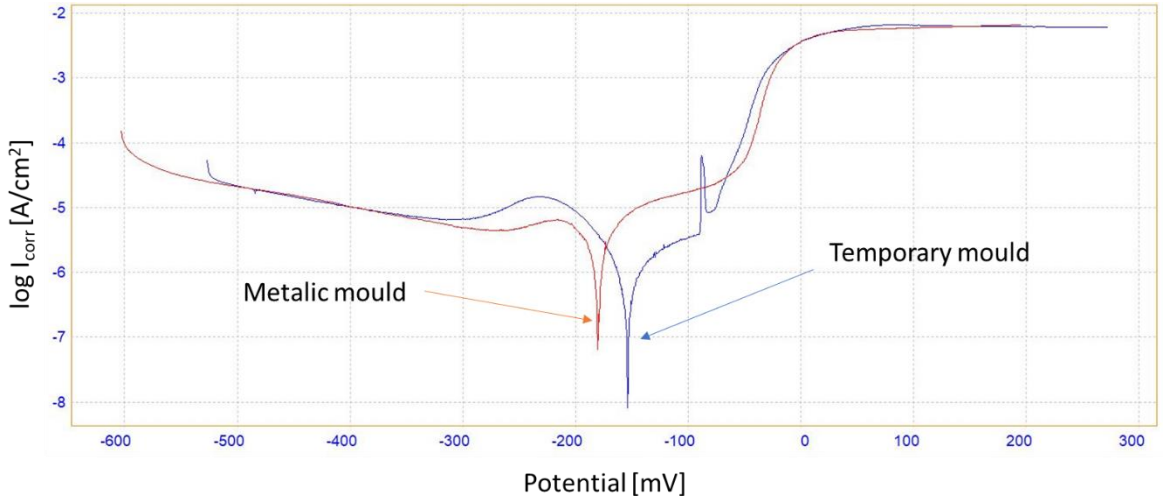

Fig. 5. Potentiodynamic polarization curves of SAE 430B alloy solidified in contact with temporary form and permanent form

As can be seen from Table 3, the corrosion potential values are in the negative domain. The closest value to the positive range is that of the sample solidified in contact with the temporary mould.

Table 3. Electrochemical corrosion parameters determined for SAE 430B samples cast in metallic and temporary mould in seawater corrosive media

Sample	E_{cor} (mv)	I_{cor} ($\mu A/cm^2$)	R_p ($k\Omega \cdot cm^2$)	C_R ($\mu m/an$)
Metallic mould	-180.20	5.98	3.28	69.32
Temporary mould	-153.90	1.34	9.85	15.53

Observing both, the value of the corrosion potentials and current density, it can be seen that the samples solidified into metallic mould show a higher corrosion tendency compared to the sample cast in a temporary mould. These trends are also confirmed by the polarization resistance value which is approximately 3 times lower, 3.28 $k\Omega \cdot cm^2$ in comparison to the value 9.85 $k\Omega \cdot cm^2$. The corrosion speed is approximately 4 times lower for the sample slowly solidified compared to the sample solidified at a higher speed. It is possible that this decrease in corrosion rate is due to grain boundaries areas that are much lower in the case of the sample solidified in contact with the temporary mould, which has a larger grain size compared to the solidified sample in contact with the metallic mould. Analyzing the literature, no values of corrosion process parameters were found for the alloy SAE 430B but it can be seen that, regardless of the type of structure of CuZn-based alloys, the corrosion resistance obtained in the case of the studied material is higher than the values obtained for classical alloys when the same corrosion medium was used: seawater [12]. In addition, the studies showed that the corrosion rate for classical brass in natural seatwater is 110 μm/an [13], much higher compared to that of alloy SAE 430B analyzed.

4. CONCLUSIONS

• In the case of temporary mould solidified samples, their structure consists of β phase grains and precipitates which are less numerous than metallic mould solidified samples. With increasing cooling rate, the decrease in grain size and the appearance of precipitates is favored. Casting in permanent moulds favors the appearance of α phase at the grain boundaries of β phase.
• EDS characterization shows the chemical composition of Cu-rich β and α phases as well as precipitates (Fe and Mn-rich) found in the β phase. The sample cast in metallic mould has Pb in composition, but this element is not identified in the temporary mould cast sample.
• The temporary form cast sample shows a corrosion rate of approximately 4 times lower and a corrosion resistance 3 times higher then the metallic mould cast samples. Therefore, obtaining samples by casting in permanent mould causes a higher corrosion tendency compared to casting in temporary mould.

Funding: This paper was supported by the Research contract: Research on the influence of casting conditions on the properties of SAE 430 B alloy castings ($CuZn_{25}Al_5Fe_3Mn_4$), project nr. 49104/2022.

REFERENCES

1.SR EN 1982:2008 *Copper and copper alloys. Ingots and castings*, vailable at: https://magazin.asro.ro/ro/standard/166815.
2. Dharmendra C., Hadadzadeh A., Amirkhiz B.S., Janaki Ram G.D., Mohammadi M. (2019). *Microstructural evolution and mechanical behavior of nickel aluminum bronze Cu-9Al-4Fe-4Ni-1Mn fabricated through wire-arc additive manufacturing*, Addit. Manuf., 30, 100872.
3. Song Q.N., Zhang H.N., Li H.L., Hong H., Sun S.Y., Xu N., Zhang G.Y., Bao Y.F., Qiao Y.X., (2022). *Corrosion and cavitation erosion behaviors of the manganese-aluminum-bronze cladding layer prepared by MIG in 3.5% NaCl solution*, Mater. Today Commun., 31, 103566.
4. Carcea I., Gherghe M., (2009). *Aliaje neferoase de turnatorie*, pp. 110 - 122, Performantica Publishing House, Iasi.
5. Mota N.M., Tavares S.S.M., Nascimento A.M., Zeeman G., Biezma-Moraleda M.V. (2021). *Failure analysis of a butterfly valve made with nickel aluminum Bronze (NAB) and manganese aluminum Bronze (MAB)*, Eng. Fail. Anal., 129, 105732.
6. Mirzadeh Rahni M. R., Beidokhti B., Haddad-Sabzevar M., *Effect of filler metal on microstructure and mechanical properties of manganese−aluminum bronze repair welds* (2017). Trans. Nonferrous Met. Soc. China, 27, 507−513.
7. Pranesh, Anas S. M., Johnson S., Jose R., Sachin B., Govindarajan S., Vijayan V., Karinka S., *Determining the solidification characteristics of Manganese bronze (MAB) alloy using computer-aided cooling curve analysis*, (2022). Mater. Today: Proc., 52(3), 2095-2101.

8. Yao Q., T., Huilin L., Nan X.., Chenbo X., Ye-feng B., Li Y., YQiao. X., (2020). *Friction stir processing of a cast manganese-aluminum bronze for improving corrosion and cavitation erosion resistances*. Surf. Topogr.: Metrol. Prop., 8, 025020.
9. Pugacheva N. B., Pankratov A. A., Yu N. Frolova, Kotlyarov I. V., (2006). *Structural and Phase Transformations in α + β Brasses*, Russian Metallurgy (Metally), 2006(3), 239–248.
10. Hashemi M., (2015). *Microstructure and Wear Behavior of a Manganese Bronze Bearing Material under Unlubricated Conditions*, Tribol. Trans., 58, 750–757.
11. Hashemi M., Halvaee A., *Effect of GTAW Parameters on Structure and Mechanical Properties of C86300 Weld Joint* (2014). Trans Indian Inst Met, 67(5), 741–752.
12. Santos C.I.S., Mendonca M.H., Fonseca I.T.E., (2006). *Corrosion of brass in natural and artificial seawater*, Appl. Electrochem, 36, 1353–1359.
13. Xavier J. R., Nanjundan S., Rajendran N., (2012). *Electrochemical Adsorption Properties and Inhibition of Brass Corrosion in Natural Seawater by Thiadiazole Derivatives: Experimental and Theoretical Investigation*, Ind. Eng. Chem. Res., 51, 30–43.

Received: July 17, 2023 / Accepted: December 15, 2023 / Paper available online: December 20, 2023 © International Journal of Modern Manufacturing Technologies